



31 **1. Introduction**

32 Iceberg calving is an important process that accounts for around 50% of total mass loss to the  
33 ocean in Antarctica (Depoorter et al., 2013; Rignot et al., 2013). Moreover, dynamic  
34 feedbacks associated with retreat and/or thinning of buttressing ice shelves or floating glacier  
35 tongues can result in an increased discharge of ice into the ocean (Rott et al., 2002; Rignot et  
36 al., 2004; Wuite et al., 2015; Fürst et al., 2016). At present, calving dynamics are only  
37 partially understood (Benn et al., 2007; Chapuis and Tetzlaff, 2014) and models struggle to  
38 replicate observed calving rates (van der Veen, 2002; Astrom et al., 2014). Therefore,  
39 improving our understanding of the mechanisms driving glacier calving and how glacier  
40 calving cycles have responded to recent changes in the ocean-climate system is important in  
41 the context of future ice-sheet mass balance and sea level.

42 Calving is a two-stage process that requires both the initial ice fracture and the subsequent  
43 transport of the detached iceberg away from the calving front (Bassis and Jacobs, 2013). In  
44 Antarctica, major calving events can be broadly classified into two categories: the discrete  
45 detachment of large tabular icebergs (e.g. Mertz glacier tongue: Massom et al., 2015) or the  
46 spatially extensive disintegration of floating glacier tongues or ice shelves into numerous  
47 smaller icebergs (e.g. Larsen A & B ice shelves Rott et al., 1996; Scambos et al., 2009).  
48 Observations of decadal-scale changes in glacier terminus position in both the Antarctic  
49 Peninsula and East Antarctica have suggested that despite some degree of stochasticity,  
50 iceberg calving and glacier advance/retreat is likely driven by external climatic forcing (Cook  
51 et al., 2005; Miles et al., 2013). However, despite some well-documented ice-shelf collapses  
52 (Scambos et al., 2003; Banwell et al., 2013) and major individual calving events (Masson et  
53 al., 2015) there is a paucity of data on the nature and timing of calving from glaciers in  
54 Antarctica (e.g. compared to Greenland: Moon and Joughin, 2008; Carr et al., 2013), and  
55 particularly in East Antarctica.

56 Following recent work that highlighted the potential vulnerability of the East Antarctic Ice  
57 Sheet in Wilkes Land to ocean-climate forcing and marine ice-sheet instability (Greenbaum  
58 et al., 2015; Aitken et al., 2016; Miles et al., 2013; 2016), we analyse the recent calving  
59 activity of six outlet glaciers in the Porpoise Bay region using monthly satellite imagery  
60 between November 2002 and March 2012. In addition, we also observe the start of a large  
61 calving event in 2016. We then turn our attention to investigating the drivers behind the  
62 observed calving dynamics.

## 63        **2. Study area**

64    Porpoise Bay (76°S, 128°E) is situated in Wilkes Land, East Antarctica, approximately 300  
65    km east of Moscow University Ice Shelf and 550 km east of Totten glacier (Fig. 1). This area  
66    was selected for study because it occupies a central position in Wilkes Land, which is thought  
67    to have experienced mass loss over the past decade (King et al., 2012; Sasgen et al., 2013;  
68    McMillan et al., 2014), and which is the only region of East Antarctica where the majority of  
69    marine-terminating outlet glaciers have experienced recent (2000-2012) retreat (Miles et al.,  
70    2016). This is particularly concerning because Wilkes Land overlies the Aurora Subglacial  
71    Basin and, due its reverse bed slope and deep troughs (Young et al., 2011), it may have been  
72    susceptible to unstable grounding line retreat in the past (Cook et al., 2014), and could make  
73    significant contributions to global sea level in the future (DeConto and Pollard, 2016).  
74    However, despite some analysis on glacier terminus position on decadal timescales (Frezzotti  
75    and Polizzi, 2002; Miles et al., 2013; 2016), there has yet to be any investigation of inter-  
76    annual and sub-annual changes in terminus position and calving activity in the region.

77    Porpoise Bay is 150 km wide and is typically filled with landfast multi-year sea ice (Fraser et  
78    al., 2012). In total, six glaciers were analysed, with glacier velocities (from Rignot et al.,  
79    2011) ranging from ~440 m yr<sup>-1</sup> (Sandford Glacier) to ~2000 m yr<sup>-1</sup> (Frost Glacier). Recent  
80    studies have suggested that the largest (by width) glacier feeding into the bay - Holmes  
81    Glacier - has been thinning over the past decade (Pritchard et al., 2009; McMillan et al.,  
82    2014).

## 83        **3. Methods**

### 84        **3.1 Satellite imagery and terminus position change**

85    Glacier terminus positions were mapped at approximately monthly intervals between  
86    November 2002 and March 2012, using Envisat Advanced Synthetic Aperture Radar (ASAR)  
87    Wide Swath Mode (WSM) imagery across six glaciers, which were identified from the  
88    Rignot et al. (2011b) ice-velocity dataset (Fig.1). Additional sub-monthly imagery between  
89    December 2006 and April 2007 were used to gain a higher temporal resolution following the  
90    identification of a major calving event around that time. During the preparation for this  
91    manuscript we also observed the start of another large calving event with Sentinel-1 imagery  
92    (Table 1).

93 Approximately 65% of all glacier frontal measurements were made using an automated  
94 mapping method. This was achieved by automatically classifying glacier tongues and sea ice  
95 into polygons based on their pixel values, with the boundary between the two taken as the  
96 terminus position. The threshold between glacial ice and sea ice was calculated automatically  
97 based on the image pixel statistics, whereby sea ice appears much darker than the glacial ice.  
98 In images where the automated method was unsuccessful, terminus position was mapped  
99 manually. The majority of these manual measurements were undertaken in the austral  
100 summer (December – February) when automated classification was especially problematic  
101 due to the high variability in backscatter on glacier tongues as a result of surface melt.  
102 Following the mapping of the glacier termini, length changes were calculated using the box  
103 method (Moon and Joughin, 2008). This method calculates the glacier area change between  
104 each time step divided by the width of the glacier, to give an estimation of glacier length  
105 change. The width of glacier was obtained by a reference box which approximately delineates  
106 the sides of the glacier.

107 Given the nature of the heavily fractured glacier fronts and the moderate resolution of Envisat  
108 ASAR WSM imagery (80 m) it was sometimes difficult to establish whether individual or  
109 blocks of icebergs were attached to the glacier tongue. As a result, there are errors in  
110 precisely determining terminus change on a monthly time-scale ( $\sim\pm$  500 m). However,  
111 because our focus is on major calving events, absolute terminus position is less important  
112 than the identification of major episodes of calving activity. Indeed, because estimations of  
113 terminus position were made at approximately monthly intervals, calving events were easily  
114 distinguished because the following month's estimation of terminus position would clearly  
115 show the glacier terminus in a retreated position. In addition, each image was also checked  
116 visually to make sure no small calving events were missed (i.e. as indicated by the presence  
117 of icebergs proximal to the glacier tongue).

### 118 **3.2 Sea ice**

119 Sea ice concentrations in Porpoise Bay were calculated using mean monthly Bootstrap sea ice  
120 concentrations derived from the Nimbus-7 satellite and the Defence Meteorological Satellite  
121 Program (DMSP) satellites which offers near complete coverage between October 1978 and  
122 December 2014 (Comiso, 2014; <http://dx.doi.org/10.5067/J6JQLS9EJ5HU>). To extend the  
123 sea ice record, we also use mean monthly Nimbus-5 Electrically Scanning Microwave  
124 Radiometer (ESMR) derived sea ice concentrations (Parkinson et al., 2004;

125 [https://nsidc.org/data/docs/daac/nsidc0009\\_esmr\\_seaice.gd.html](https://nsidc.org/data/docs/daac/nsidc0009_esmr_seaice.gd.html)), which offer coverage  
126 between December 1972 and March 1977. However, from March to May 1973, August 1973,  
127 April 1974 and June to August 1975, mean monthly sea ice concentrations were not  
128 available. Sea ice concentrations were extracted from 18 grid cells, covering 11,250 km<sup>2</sup>  
129 across Porpoise Bay, but not into the extended area beyond the limits of the bay (Fig. 1). Grid  
130 cells which were considered likely to be filled with glacial ice were excluded. Pack-ice  
131 concentrations were also extracted from a 250 x 150 km polygon adjacent to Porpoise Bay.  
132 The dataset has a spatial resolution of 25 km and monthly sea ice concentration anomalies  
133 were calculated from the 1972-2016 monthly mean.

134 Daily sea ice concentrations derived from the Artist Sea ice (ASI) algorithm from Advanced  
135 Microwave Scanning Radiometer - EOS (AMSR-E) data (Spren et al., 2008) were used to  
136 calculate daily sea ice concentration anomalies during the January 2007 sea ice break-up  
137 (<http://icdc.zmaw.de/1/daten/cryosphere/seaiceconcentration-asi-amsre.html>). This dataset  
138 was used because it provides a higher spatial resolution (6.25 km) compared to those  
139 available using Bootstrap derived concentrations (25 km). This is important because it  
140 provides a more accurate representation of when sea ice break-up was initiated and, due to its  
141 much higher spatial resolution, it provides data from much closer to the glacier termini (see  
142 Fig.1).

### 143 **3.3 RACMO**

144 We used the Regional Atmospheric Climate Model (RACMO) V2.3 (van Wessem et al., 2014)  
145 to simulate daily surface melt fluxes in the study area between 1979 and 2015 at a 27 km  
146 spatial resolution. The melt values were extracted from floating glacier tongues in Porpoise  
147 Bay because the model masks out sea ice, equating to seven grid points. The absolute surface  
148 melt values are likely to be different on glacial ice, compared to the sea ice, but the relative  
149 magnitude of melt is likely to be similar temporally.

### 150 **3.4 ERA-Interim**

151 In the absence of weather stations in the vicinity of Porpoise Bay we use the 0.25° ERA-  
152 Interim reanalysis dataset ([http://apps.ecmwf.int/datasets/data/interim-full-](http://apps.ecmwf.int/datasets/data/interim-full-modala/levtype=sfc/)  
153 [modala/levtype=sfc/](http://apps.ecmwf.int/datasets/data/interim-full-modala/levtype=sfc/)) to calculate mean monthly wind-field and sea-surface temperature (SST)  
154 anomalies, with respect to the 1979-2015 monthly mean. Wind-field anomalies were  
155 calculated by using the mean monthly 10 m zonal (U) and meridional (V) wind components.

156 We also used the daily 10 m zonal (U) and meridional (V) components to simulate wind-field  
157 vectors in Porpoise Bay on January 11<sup>th</sup> 2007 and March 19<sup>th</sup> 2016 which are the estimated  
158 dates of sea ice break-up.

## 159 **4. Results**

### 160 **4.1 Terminus position change**

161 Analysis of glacier terminus position change of six glaciers in Porpoise Bay between  
162 November 2002 and March 2012 reveals three broad patterns of glacier change (Fig. 2). The  
163 first pattern is shown by Holmes (West) Glacier, which advances a total of ~13 km throughout  
164 the observation period, with no evidence of any major iceberg calving that resulted in  
165 substantial retreat of the terminus beyond the measurement error (+/- 500 m). The second is  
166 shown by Sandford Glacier tongue, which advanced ~1.5 km into the ocean between  
167 November 2002 and April 2006, before its floating tongue broke away in May 2006. A further  
168 smaller calving event was observed in January 2009. Overall, by the end of the study period,  
169 its terminus had retreated around 1 km from its position in November 2002. The third pattern is  
170 shown by Frost Glacier, Glacier 1, Glacier 2 and Holmes (East) Glaciers, which all advanced  
171 between November 2002 and January 2007, albeit with a small calving event in Frost Glacier  
172 in May 2006. However, between January and April 2007, Frost Glacier, Glacier 1, Glacier 2  
173 and Holmes (East) Glaciers all underwent a large near-simultaneous calving event. This led to  
174 1,300 km<sup>2</sup> of ice being removed from glaciers in Porpoise Bay, although we also note the  
175 disintegration of a major tongue from an unnamed glacier further west, which contributed a  
176 further 1,600 km<sup>2</sup>. Thus, in a little over three months, a total of 2,900 km<sup>2</sup> of ice was removed  
177 from glacier tongues in the study area (Fig. 3). Following this calving event, the fronts of these  
178 glaciers stabilised and began advancing at a steady rate until the end of the study period  
179 (March, 2012) (Fig. 2), with the exception of Frost Glacier which underwent a small calving  
180 event in April 2010.

### 181 **4.2 Evolution of the 2007 calving event**

182 A series of eight sub-monthly images between December 11<sup>th</sup> 2006 and April 8<sup>th</sup> 2007 shows  
183 the evolution of the 2007 calving event (Fig. 4). Between December 11<sup>th</sup> 2006 and January 2<sup>nd</sup>  
184 2007, the landfast sea ice edge retreats past Sandford Glacier to the edge of Frost Glacier and  
185 there is some evidence of sea ice fracturing in front of the terminus of Glacier 2 (Fig. 4b).  
186 From January 2<sup>nd</sup> to January 9<sup>th</sup> a small section (~40 km<sup>2</sup>) of calved ice broke away from Frost

187 Glacier, approximately in line with the retreat edge of landfast sea ice (Fig. 4c). By January  
188 25<sup>th</sup>, significant fracturing in the landfast sea ice had developed, and detached icebergs from  
189 Frost, Glaciers 1, Glacier 2 and Holmes (East) Glaciers begin to breakaway (Fig. 4d). This  
190 process of rapid sea ice breakup in the east section of the bay and the disintegration of sections  
191 of Frost glacier, Glacier 1, Glacier 2 and Holmes (East) Glaciers continues up to March 10<sup>th</sup>  
192 2007 (Fig. 4g). In contrast, the west section of Porpoise Bay remains covered in sea ice in front  
193 of Holmes (West) Glacier, which does not calve throughout this event. By April 8<sup>th</sup>, the  
194 calving event had ended with a large number of calved icebergs now occupying the bay (Fig.  
195 4h).

### 196 **4.3 2016 calving event**

197 During the preparation of this manuscript satellite observations of Porpoise Bay revealed that  
198 another large near-simultaneous disintegration of glacier tongues in Porpoise Bay was  
199 currently underway. This event was initiated on March 19<sup>th</sup> where the edge of the multi-year  
200 sea ice retreated to the Holmes (West) Glacier terminus, removing multi-year sea ice which  
201 was at least 14 years old. By March 24<sup>th</sup> this had led to the rapid disintegration of an 800 km<sup>2</sup>  
202 section of the Holmes (West) Glacier tongue (Fig. 5). This was the first observed calving of  
203 Holmes (West) glacier at any stage between November 2002 and March 2016. Throughout  
204 March and April the break-up of sea ice continued and by May 13<sup>th</sup> it had propagated to the  
205 terminus of Frost Glacier, resulting in the disintegration of large section of its tongue (Fig. 6).  
206 By 24<sup>th</sup> July sea ice had been removed from all glacier termini in Porpoise Bay at some point  
207 during the event, resulting in a total of ~2,200 km<sup>2</sup> ice being removed from glacier tongues  
208 (Fig. 6).

### 209 **4.4. The link between sea ice and calving in Porpoise Bay**

210 Analysis of mean monthly sea ice concentration anomalies in Porpoise Bay between  
211 November 2002 and June 2016 (Fig. 7) reveals a major negative sea ice anomaly occurred  
212 between January and June 2007, where monthly sea ice concentrations were between 35%  
213 and 40% below average. This is the only noticeable (>20%) negative ice anomaly in Porpoise  
214 Bay and it coincides with the major January 2007 calving event (see Fig. 4). However,  
215 despite satellite imagery showing the break-up of sea ice prior to the 2016 calving event (Fig.  
216 5 and 6), in a similar manner to that in 2007 (e.g. Fig. 4), no large negative anomaly is  
217 present in the sea ice concentration data. This is likely to reflect the production of a large  
218 armada of icebergs following the disintegration of Holmes (West) Glacier (e.g. Fig. 6),

219 helping to promote a rapid sea ice reformation in the vicinity of Porpoise Bay. Furthermore,  
220 we note that the smaller calving events of Sandford and Frost Glaciers all take place after sea  
221 ice had retreated away from the glacier terminus (Fig. 8). Indeed, throughout the study  
222 period, there is no evidence of any calving events taking place with sea ice proximal to  
223 glacier termini. This suggests that glaciers in Porpoise Bay are very unlikely to calve with sea  
224 ice present at their termini.

#### 225 **4.5. Atmospheric circulation anomalies**

226 Atmospheric circulation anomalies in the months preceding the January 2007 and March  
227 2016 sea ice break-ups reveal contrasting conditions. In the austral summer which preceded  
228 the January 2007 break-up there were strong positive SST anomalies and atmospheric-  
229 circulation anomalies throughout December 2005 (Fig. 9a). The circulation anomaly was  
230 reflected in a strong easterly airflow offshore from Porpoise Bay. This is associated with a  
231 band of cooler SSTs close to the coastline and the northward shift of the Antarctic Coastal  
232 Current in response to the weakened westerlies (e.g. Langlais et al., 2015). A weakened zonal  
233 flow combined with high SST in the South Pacific would allow the advection of warmer  
234 maritime air into Porpoise Bay. Consistent with warmer air are estimates of exceptionally  
235 high melt values in Porpoise Bay during December 2005 derived from the RACMO2.3,  
236 which contrasts with the longer-term trend of cooling (Fig. 10). However, the December  
237 2005 anomaly was short lived and, by January 2006, the wind-field conditions were close to  
238 average, although SST remained slightly higher than average (Fig. 9b).

239 In December 2006 and January 2007, which are the months immediately before and during  
240 the break-up of sea ice, atmospheric conditions were close to average, with very little  
241 deviation from mean conditions in the wind field and a small negative SST anomaly (Fig.  
242 9c). However, on January 11<sup>th</sup> 2007, which is the estimated date of sea ice break-up from  
243 AMSR-E data, we note that there were very high winds close to Porpoise Bay (Fig. 11a).

244 In contrast to the months preceding the January 2007 event, we find little deviation from  
245 average conditions prior to the March 2016 break-up event. In the austral summer which  
246 preceded the 2016 break-up (2014/15), there was little deviation from the average wind field  
247 and only a small increase from average SSTs (Fig 9d). In December and January 2015/16,  
248 there was evidence for a small increase in the strength of westerly winds, and cooler SSTs in  
249 the South Pacific (Fig. 9e). However, in February and March 2016 there was no change from  
250 the average wind field and slightly cooler SSTs (Fig. 9f). We note, however, that there was a



251 low pressure system passing across Porpoise Bay on March 19<sup>th</sup> 2016, the estimated date of  
252 break-up initiation (Fig. 11b).

#### 253 **4.6 Holmes (West) Glacier calving cycle**

254 Through mapping the terminus position in all available satellite imagery (Table 1) dating  
255 back to 1963, we are able to reconstruct large calving events on the largest glacier in Porpoise  
256 bay, Holmes (West) (Fig. 12). On the basis that a large calving event is likely during the  
257 largest sea ice break-up events, we estimate the date of calving based on sea ice  
258 concentrations in Porpoise Bay when satellite imagery is not available. Our estimates suggest  
259 that Holmes (West) Glacier calves at approximately the same position in each calving cycle,  
260 including the most recent calving event in March 2016.

### 261 **5. Discussion**

#### 262 **5.1 Sea ice break-up and the disintegration of glacier tongues in Porpoise Bay**

263 We report a major, near-synchronous calving event in January 2007 and a similar event that  
264 was initiated in 2016. This resulted in  $\sim 2,900 \text{ km}^2$  and  $2,200 \text{ km}^2$  of ice respectively, being  
265 removed from glacier tongues in the Porpoise Bay region of East Antarctica. These calving  
266 events are comparable to some of the largest disintegration events ever observed in Antarctica  
267 (e.g. Larsen A in 1995,  $4,200 \text{ km}^2$  and Larsen B in 2002,  $3,250 \text{ km}^2$ ); and is the largest event to  
268 have been observed in East Antarctica. However, they differ from those observed on the ice  
269 shelves of the Antarctic Peninsula, in that they may be more closely linked to a cycle of glacier  
270 advance and retreat, as opposed to a catastrophic collapse that may be unprecedented.

271 Given the correspondence between the sea ice and glacier-terminus changes, we suggest that  
272 these disintegration events were driven by the break-up of the multi-year landfast sea ice which  
273 usually occupies Porpoise Bay and the subsequent loss of buttressing of the glacier termini. A  
274 somewhat similar mechanism has been widely documented in Greenland, where the dynamics  
275 of sea ice melange in proglacial fjords have been linked to inter-annual variations in glacier  
276 terminus position (Amundson et al., 2010; Carr et al., 2013; Todd and Christoffersen, 2014;  
277 Cassotto et al., 2015). Additionally, the mechanical coupling between thick multi-year landfast  
278 sea ice and glacier tongues may have acted to stabilize and delay the calving of the Mertz  
279 Glacier tongue (Massom et al., 2010) and Brunt/Stancomb-Wills Ice Shelf system (Khazendar  
280 et al., 2009). However, this is the first observational evidence directly linking multi-year  
281 landfast sea ice break-up to the large-scale and rapid disintegration of glacier tongues. This is

282 important because landfast sea ice is highly sensitive to climate (Heil, 2006; Mahoney et al.,  
283 2007) and, if future changes in climate were to result in a change to the persistence and/or  
284 stability of the landfast ice in Porpoise Bay, it may result in detrimental effects on glacier  
285 tongue stability. An important question, therefore, is: what process(es) cause sea ice break-up?

## 286 **5.2 What caused the January 2007 and March 2016 sea ice break-ups?**

287 The majority of sea ice in Porpoise Bay is multi-year sea ice (Fraser et al., 2012), and it is  
288 likely that various climatic processes operating over different timescales contributed to the  
289 January 2007 sea ice break-up event. Although there are no long-term observations of multi-  
290 year sea ice thickness in Porpoise Bay, observations and models of the annual cycle of multi-  
291 year sea ice in other regions of East Antarctica suggest that multi-year sea ice thickens  
292 seasonally and thins each year (Lei et al., 2010; Sugimoto et al., 2016; Yang et al., 2016).  
293 Therefore, the relative strength, stability and thickness of multi-year sea ice over a given  
294 period is driven not only by synoptic conditions in the short term (days/weeks), but also by  
295 climatic conditions in the preceding years.

296 In the austral summer (2005/06) which preceded the break-up event in January 2007, there was  
297 a strong easterly airflow anomaly throughout December 2005 directly adjacent to Porpoise Bay  
298 (Fig. 9a). This anomaly represents the weakening of the band of westerly winds which encircle  
299 Antarctica, and is reflected in an exceptionally negative Southern Annular Mode (SAM) index  
300 in December 2005 (Marshall, 2003). This contrasts with the long-term trend for a positive  
301 SAM index (Marshall, 2007; Miles et al., 2013). A weaker band of westerly winds combined  
302 with anomalously high SST in the Southern Pacific (Fig. 9a) would allow a greater advection  
303 of warmer maritime air towards Porpoise Bay. Indeed, RACMO2.3-derived surface-melt  
304 estimates place December 2005 as the second highest mean melt month (1979-2015) on the  
305 modelled output in Porpoise Bay (Fig. 10). To place this month into perspective, we note that it  
306 would rank above the average melt values of all Decembers and Januarys since 2000 on the  
307 remnants of Larsen B Ice Shelf. Comparing MODIS satellite imagery from before and after  
308 December 2005 reveals the development of significant fracturing in the multi-year sea ice (Fig  
309 13a, b). These same fractures remain visible prior to the break-out event in January 2007 and,  
310 when the multi-year sea ice begins to break-up, it ruptures along these pre-existing weaknesses  
311 (Fig. 13c). As such, this strongly suggests that the atmospheric-circulation anomalies of  
312 December 2005 played an important role in the January 2007 multi-year sea ice break-up and  
313 near-simultaneous calving event.

314 The break-up of landfast sea ice has been linked to dynamic wind events and ocean swell  
315 (Heil, 2006; Ushio, 2006; Fraser et al., 2012). Thus, it is possible that the wind anomalies in  
316 December 2005 may have been important in initiating the fractures observed in the sea ice in  
317 Porpoise Bay, through changing the direction and/or intensity of oceanic swell. However, this  
318 mechanism is thought to be at its most potent during anomalously low pack-ice concentrations  
319 because pack ice can act as a buffer to any oceanic swell (Langhorne et al., 2001; Heil, 2006;  
320 Fraser, 2012). That said, we note that pack-ice concentrations offshore from Porpoise Bay  
321 were around average during December 2005 (Fig. 7). This may suggest that there are other  
322 mechanisms that were important in the weakening of the multi-year sea ice in Porpoise Bay in  
323 December 2005.

324 In the Arctic, sea ice melt-ponding along pre-existing weaknesses has been widely reported to  
325 precede sea ice break-up (Ehn et al., 2011; Petrich et al., 2012; Landy et al., 2014; Schroder et  
326 al., 2014; Arntsen et al., 2015). Despite its importance in the Arctic, it has yet to be considered  
327 as a possible factor in landfast sea ice break-up in coastal Antarctica. As a consequence of the  
328 high melt throughout December 2005, the growth of sea ice surface ponding would be  
329 expected, in addition to surface thinning of the sea ice. High-resolution cloud-free optical  
330 satellite coverage of Porpoise Bay throughout December 2005 is limited, but ASTER imagery  
331 in the vicinity of Frost Glacier on the 4<sup>th</sup> and 31<sup>st</sup> December 2005 shows surface melt features  
332 and the development of fractures throughout the month (Fig. 13d,e), similar to those observed  
333 elsewhere in East Antarctica (Kingslake et al., 2015; Langley et al., 2016). High-resolution  
334 imagery from 16<sup>th</sup> January 2006 (via GoogleEarth) shows the development of melt ponds on  
335 the sea ice surface (Fig. 13f). Therefore, it is possible that surface melt had some impact on the  
336 fracturing of landfast sea ice in Porpoise Bay. This may have caused hydro-fracturing of pre-  
337 existing depressions in the landfast ice or surface thinning may have made it more vulnerable  
338 to fracturing through ocean swell or internal stresses. Additionally, the subsequent refreezing  
339 of some melt ponds may temporarily inhibit basal ice growth, potentially weakening the multi-  
340 year sea ice and predisposing it to future break-up (Flocco et al., 2015). It is important to note  
341 that the atmospheric circulation anomalies which favoured the development of fractures in the  
342 multi-year sea ice in December 2005 were short-lived. By January 2006, atmospheric  
343 conditions had returned close to average (Fig. 9b) and remained so until the austral winter,  
344 where sea ice break-up is less likely. This may explain the lag between the onset of sea ice  
345 fracturing in December 2005 and its eventual break-up in the following summer (January  
346 2007).

347 Consistent with the notion that the multi-year sea ice was already in a weakened state prior to  
348 its break-up in 2007, is that the break-up occurred in January, several weeks before the likely  
349 annual minima in multi-year sea ice thickness (Yang et al., 2016; Lei et al., 2010) and landfast  
350 ice extent (Fraser et al., 2012). Additionally, atmospheric circulation anomalies indicate little  
351 deviation from average conditions in the immediate months preceding break-up (Fig. 9b, c),  
352 suggesting that atmospheric conditions were favourable for sea ice stability. Despite this, a  
353 synoptic event is still likely required to force the break-up in January 2007. Daily sea ice  
354 concentrations in Porpoise Bay in January 2007 show a sharp decrease in sea ice  
355 concentrations after 12<sup>th</sup> January, representing the onset of sea ice break-out (Fig 14). This is  
356 preceded by a strong melt event recorded by the RACMO2.3 model, centred on January 11<sup>th</sup>,  
357 which may represent a low-pressure system. Indeed, ERA-Interim estimates of the wind field  
358 suggest strong south-easterly winds in the vicinity of Porpoise Bay (Fig 11 a). Unlike in  
359 December 2005, pack-ice concentrations offshore of Porpoise Bay were anomalously low (Fig.  
360 7). Therefore, with less pack-ice buttressing, it is possible that the melt event, high winds and  
361 associated ocean swell may have initiated the break-up of the already weakened multi-year sea  
362 ice in Porpoise Bay.

363 In contrast to January 2007, we find no link between atmospheric-circulation anomalies and  
364 the March 2016 sea ice break-up. In the preceding months to the March 2016 break-up, wind  
365 and SST anomalies indicate conditions close to average conditions favouring sea ice stability  
366 (Fig. 9 d, e, f). This suggests another process was important in driving the March 2016 sea ice  
367 break-up. A key difference between the 2007 and 2016 event is that the largest glacier in the  
368 bay, Holmes (West) Glacier, only calved in the 2016 event. Analysis of its calving cycle (Fig.  
369 12) indicates that it calves at roughly the same position in each cycle and that its relative  
370 position in early 2016 suggests that calving was ‘overdue’ (Fig. 12). This indicates that the  
371 calving cycle of Holmes (West) Glacier has not necessarily been driven by atmospheric  
372 circulation anomalies. Instead, we suggest that as Holmes (West) Glacier advances, it slowly  
373 pushes the multi-year sea ice attached to its terminus further towards the open ocean to the  
374 point where the sea ice attached to the glacier tongue becomes more unstable. This could be  
375 influenced by local bathymetry and oceanic circulation, but no observations are available.  
376 However, once the multi-year sea ice reaches an unstable state, break-up is still likely to be  
377 forced by a synoptic event. This is consistent with our observations, where ERA-Interim  
378 derived wind fields show the presence of a low-pressure system close to Porpoise Bay on the  
379 estimated date of sea ice break-up in March 2016 (Fig. 11 b). Whilst we suggest that the

380 March 2016 sea ice break-up and subsequent calving of Holmes (West) are currently part of a  
381 predictable cycle, we note that this could be vulnerable to change if any future changes in  
382 climate alter the persistence and/or strength of the multi-year sea ice, which is usually  
383 attached to the glacier terminus.

## 384 **6. Conclusion**

385 We identify two large near-simultaneous calving events in January 2007 and March 2016  
386 which were driven by the break-up of the multi-year landfast sea ice which usually occupies  
387 the bay. This provides a previously unreported mechanism for the rapid disintegration of  
388 floating glacier tongues in East Antarctica, adding to the growing body of research linking  
389 glacier tongue stability to the mechanical coupling of landfast ice (e.g. Khazander et al.,  
390 2009; Massom et al., 2010). Our results suggest that multi-year sea ice break-ups in 2007 and  
391 2016 in Porpoise Bay were driven by different mechanisms. We link the 2007 event to  
392 atmospheric-circulation anomalies in December 2005 weakening multi-year sea ice through a  
393 combination of surface melt and a change in wind direction, prior to its eventual break-up in  
394 2007. This is in contrast to the March 2016 event, which we suggest is part of a longer-term  
395 cycle based on the terminus position of Holmes (West) Glacier that was able to advance and  
396 push sea ice out of the bay. The link between sea ice break-up and major calving of glacier  
397 tongues is especially important because it suggests that with predictions of future warming  
398 (DeConto and Pollard, 2016) multi-year landfast ice may become less persistent. Therefore,  
399 the glacier tongues which depend on landfast ice for stability may become less stable in the  
400 future. In a wider context, our results also highlight the complex nature of the mechanisms  
401 which drive glacier calving position in Antarctica. Whilst regional trends in terminus position  
402 can be driven by ocean-climate-sea ice interaction (e.g. Miles et al., 2013; 2016), individual  
403 glaciers and individual calving events have the potential to respond differently to similar  
404 climatic forcing.

405

406 **Acknowledgements:** We thank the ESA for providing Envisat ASAR WSM data (Project ID:  
407 16713) and Sentinel data. Landsat imagery was provided free of charge by the U.S. Geological  
408 Survey Earth Resources Observation Science Centre. We thank M. van den Broeke for  
409 providing data and assisting with RACMO. B.W.J.M was funded by a Durham University  
410 Doctoral Scholarship program. S.S.R.J. was supported by Natural Environment Research  
411 Council Fellowship NE/J018333/1. We would like to thank Allen Pope and Ted Scambos for

412 reviewing the manuscript, along with the editor, Rob Bingham, for providing constructive  
413 comments which led to improvement of this manuscript.

414

## 415 **References**

- 416 Aitken, A. R. A., Roberts, J. L., van Ommen, T. D., Young, D. A., Golledge, N. R.,  
417 Greenbaum, J. S., Blankenship, D. D., and Siegert, M. J.: Repeated large-scale retreat and  
418 advance of Totten Glacier indicated by inland bed erosion, *Nature*, 533, 385-+,  
419 10.1038/nature17447, 2016.
- 420 Amundson, J. M., Fahnestock, M., Truffer, M., Brown, J., Luthi, M. P., and Motyka, R. J.: Ice  
421 melange dynamics and implications for terminus stability, Jakobshavn Isbrae Greenland, *J*  
422 *Geophys Res-Earth*, 115, Artn F01005 Doi 10.1029/2009jf001405, 2010.
- 423 Arntsen, A. E., Song, A. J., Perovich, D. K., and Richter-Menge, J. A.: Observations of the  
424 summer breakup of an Arctic sea ice cover, *Geophys Res Lett*, 42, 8057-8063,  
425 10.1002/2015GL065224, 2015.
- 426 Astrom, J. A., Vallot, D., Schafer, M., Welty, E. Z., O'Neel, S., Bartholomaeus, T. C., Liu, Y.,  
427 Riikila, T. I., Zwinger, T., Timonen, J., and Moore, J. C.: Termini of calving glaciers as self-  
428 organized critical systems, *Nat Geosci*, 7, 874-878, 10.1038/NGEO2290, 2014.
- 429 Banwell, A. F., MacAyeal, D. R., and Sergienko, O. V.: Breakup of the Larsen B Ice Shelf  
430 triggered by chain reaction drainage of supraglacial lakes, *Geophys Res Lett*, 40, 5872-5876,  
431 10.1002/2013GL057694, 2013.
- 432 Bassis, J. N., and Jacobs, S.: Diverse calving patterns linked to glacier geometry, *Nat Geosci*,  
433 6, 833-836, 10.1038/NGEO1887, 2013.
- 434 Benn, D. I., Warren, C. R., and Mottram, R. H.: Calving processes and the dynamics of calving  
435 glaciers, *Earth-Sci Rev*, 82, 143-179, 10.1016/j.earscirev.2007.02.002, 2007.
- 436 Cassotto, R., Fahnestock, M., Amundson, J. M., Truffer, M., and Joughin, I.: Seasonal and  
437 interannual variations in ice melange and its impact on terminus stability, Jakobshavn Isbrae,  
438 Greenland, *J Glaciol*, 61, 76-88, 10.3189/2015JoG13J235, 2015.
- 439 Chapuis, A., and Tetzlaff, T.: The variability of tidewater-glacier calving: origin of event-size  
440 and interval distributions, *J Glaciol*, 60, 622-634, 10.3189/2014JoG13J215, 2014.
- 441 Comiso, J. C.: Bootstrap Sea Ice Concentrations from Nimbus-7 SMMR and DMSP SSM/I-  
442 SSMIS. Version 2, Boulder, Colorado USA: NASA National Snow and Ice Data Center  
443 Distributed Active Archive Center., 2014.
- 444 Cook, A. J., Fox, A. J., Vaughan, D. G., and Ferrigno, J. G.: Retreating Glacier Fronts on the  
445 Antarctic Peninsula over the Past Half-Century, *Science*, 308, 541-544,  
446 10.1126/science.1104235, 2005.

447 Cook, C. P., Hill, D. J., van de Flierdt, T., Williams, T., Hemming, S. R., Dolan, A. M., Pierce,  
448 E. L., Escutia, C., Harwood, D., Cortese, G., and Gonzales, J. J.: Sea surface temperature  
449 control on the distribution of far-traveled Southern Ocean ice-rafted detritus during the  
450 Pliocene, *Paleoceanography*, 29, 533-548, Doi 10.1002/2014pa002625, 2014.

451 De Angelis, H., and Skvarca, P.: Glacier surge after ice shelf collapse, *Science*, 299, 1560-  
452 1562, DOI 10.1126/science.1077987, 2003.

453 DeConto, R. M., and Pollard, D.: Contribution of Antarctica to past and future sea-level rise,  
454 *Nature*, 531, 591-+, 10.1038/nature17145, 2016.

455 Depoorter, M. A., Bamber, J. L., Griggs, J. A., Lenaerts, J. T. M., Ligtenberg, S. R. M., van  
456 den Broeke, M. R., and Moholdt, G.: Calving fluxes and basal melt rates of Antarctic ice  
457 shelves, *Nature*, 502, 89-+, Doi 10.1038/Nature12567, 2013.

458 Ehn, J. K., Mundy, C. J., Barber, D. G., Hop, H., Rosnagel, A., and Stewart, J.: Impact of  
459 horizontal spreading on light propagation in melt pond covered seasonal sea ice in the  
460 Canadian Arctic, *J Geophys Res-Oceans*, 116, Artn C00g02 10.1029/2010jc006908, 2011.

461 Flocco, D., Feltham, D. L., Bailey, E., and Schroeder, D.: The refreezing of melt ponds on  
462 Arctic sea ice, *J Geophys Res-Oceans*, 120, 647-659, 10.1002/2014JC010140, 2015.

463 Fraser, A. D., Massom, R. A., Michael, K. J., Galton-Fenzi, B. K., and Lieser, J. L.: East  
464 Antarctic Landfast Sea Ice Distribution and Variability, 2000-08, *J Climate*, 25, 1137-1156,  
465 10.1175/Jcli-D-10-05032.1, 2012.

466 Frezzotti, M., and Polizzi, M.: 50 years of ice-front changes between the Adelie and Banzare  
467 Coasts, East Antarctica, *Ann Glaciol*, 34, 235-240, 10.3189/172756402781817897, 2002.

468 Fürst, J.J., Durand, G., Gillet-Chaulet, F., Tavard, L., Rankl, M., Braun, M., and Gagliardini,  
469 O.: The safety band of Antarctic ice shelves. *Nature. Clim. Chan.*, 6, 479-481, 2016.

470 Greenbaum, J. S., Blankenship, D. D., Young, D. A., Richter, T. G., Roberts, J. L., Aitken, A.  
471 R. A., Legresy, B., Schroeder, D. M., Warner, R. C., van Ommen, T. D., and Siegert, M. J.:  
472 Ocean access to a cavity beneath Totten Glacier in East Antarctica, *Nat Geosci*, 8, 294-298,  
473 10.1038/NGEO2388, 2015.

474 Heil, P.: Atmospheric conditions and fast ice at Davis, East Antarctica: A case study, *J*  
475 *Geophys Res-Oceans*, 111, Artn C05009 10.1029/2005jc002904, 2006.

476 Khazendar, A., Rignot, E., and Larour, E.: Roles of marine ice, rheology, and fracture in the  
477 flow and stability of the Brunt/Stancomb-Wills Ice Shelf, *J Geophys Res-Earth*, 114, Artn  
478 F04007 10.1029/2008jf001124, 2009.

479 Kim, K., Jezek, K. C., and Liu, H.: Orthorectified image mosaic of Antarctica from 1963  
480 Argon satellite photography: image processing and glaciological applications, *Int J Remote*  
481 *Sens*, 28, 5357-5373, 2007.

482 King, M. A., Bingham, R. J., Moore, P., Whitehouse, P. L., Bentley, M. J., and Milne, G. A.:  
483 Lower satellite-gravimetry estimates of Antarctic sea-level contribution, *Nature*, 491, 586-+,  
484 Doi 10.1038/Nature11621, 2012.

485 Kingslake, J., Ng, F., and Sole, A.: Modelling channelized surface drainage of supraglacial  
486 lakes. *J. Glaciol.*, 61 (225), 185-199, 2015.

487 Landy, J., Ehn, J., Shields, M., and Barber, D.: Surface and melt pond evolution on landfast  
488 first-year sea ice in the Canadian Arctic Archipelago, *J Geophys Res-Oceans*, 119, 3054-3075,  
489 10.1002/2013JC009617, 2014.

490 Langhorne, P. J., Squire, V. A., Fox, C., and Haskell, T. G.: Lifetime estimation for a land-fast  
491 ice sheet subjected to ocean swell, *Annals of Glaciology*, Vol 33, 33, 333-338, Doi  
492 10.3189/172756401781818419, 2001.

493 Langlais, C. E., Rintoul, S. R., and Zika, J. D.: Sensitivity of Antarctic Circumpolar Current  
494 Transport and Eddy Activity to Wind Patterns in the Southern Ocean, *J Phys Oceanogr*, 45,  
495 1051-1067, 10.1175/Jpo-D-14-0053.1, 2015.

496 Langley, E.S., Leeson, A.A., Stokes, C.R., and Jamieson, S.S.R.: Seasonal evolution of  
497 supraglacial lakes on an East Antarctic outlet glacier. *Geophys. Res. Lett.*, 43,  
498 doi:10.1002/2016GL069511,

499 Lei, R. B., Li, Z. J., Cheng, B., Zhang, Z. H., and Heil, P.: Annual cycle of landfast sea ice in  
500 Prydz Bay, east Antarctica, *J Geophys Res-Oceans*, 115, Artn C02006 10.1029/2008jc005223,  
501 2010.

502 Liu, H. X., and Jezek, K. C.: A complete high-resolution coastline of antarctica extracted from  
503 orthorectified Radarsat SAR imagery, *Photogramm Eng Rem S*, 70, 605-616, 2004.

504 Mahoney, A., Eicken, H., Gaylord, A. G., and Shapiro, L.: Alaska landfast sea ice: Links with  
505 bathymetry and atmospheric circulation, *J Geophys Res-Oceans*, 112, Artn C02001  
506 10.1029/2006jc003559, 2007.

507 Marshall, G. J.: Trends in the southern annular mode from observations and reanalyses, *J*  
508 *Climate*, 16, 4134-4143, Doi 10.1175/1520-0442(2003)016<4134:Titsam>2.0.Co;2, 2003.

509 Marshall, G. J.: Half-century seasonal relationships between the Southern Annular Mode and  
510 Antarctic temperatures, *Int J Climatol*, 27, 373-383, 10.1002/joc.1407, 2007.

511 Massom, R. A., Giles, A. B., Warner, R. C., Fricker, H. A., Legresy, B., Hyland, G.,  
512 Lescarmontier, L., and Young, N.: External influences on the Mertz Glacier Tongue (East  
513 Antarctica) in the decade leading up to its calving in 2010, *J Geophys Res-Earth*, 120, 490-506,  
514 10.1002/2014JF003223, 2015.

515 McMillan, M., Shepherd, A., Sundal, A., Briggs, K., Muir, A., Ridout, A., Hogg, A., and  
516 Wingham, D.: Increased ice losses from Antarctica detected by CryoSat-2, *Geophys Res Lett*,  
517 41, 3899-3905, Doi 10.1002/2014gl060111, 2014.

518 Miles, B. W. J., Stokes, C. R., Vieli, A., and Cox, N. J.: Rapid, climate-driven changes in  
519 outlet glaciers on the Pacific coast of East Antarctica, *Nature*, 500, 563-+, Doi  
520 10.1038/Nature12382, 2013.

521 Miles, B. W. J., Stokes, C. R., and Jamieson, S. S. R.: Pan-ice-sheet glacier terminus change in  
522 East Antarctica reveals sensitivity of Wilkes Land to sea ice changes, *Science Advances*, 2,  
523 10.1126/sciadv.1501350, 2016.



524 Moon, T., and Joughin, I.: Changes in ice front position on Greenland's outlet glaciers from  
525 1992 to 2007, *J Geophys Res-Earth*, 113, Artn F02022 Doi 10.1029/2007jf000927, 2008.

526 Parkinson, C. L., J. C. Comiso, and H. J. Zwally. 1999, updated 2004. *Nimbus-5 ESMR Polar*  
527 *Gridded Sea Ice Concentrations*. Edited by W. Meier and J. Stroeve. Boulder, Colorado USA:  
528 National Snow and Ice Data Center. Digital media.

529 Petrich, C., Eicken, H., Polashenski, C. M., Sturm, M., Harbeck, J. P., Perovich, D. K., and  
530 Finnegan, D. C.: Snow dunes: A controlling factor of melt pond distribution on Arctic sea ice,  
531 *J Geophys Res-Oceans*, 117, Artn C0902910.1029/2012jc008192, 2012.

532 Pritchard, H. D., Arthern, R. J., Vaughan, D. G., and Edwards, L. A.: Extensive dynamic  
533 thinning on the margins of the Greenland and Antarctic ice sheets, *Nature*, 461, 971-975,  
534 10.1038/nature08471, 2009.

535 Rignot, E., Casassa, G., Gogineni, P., Krabill, W., Rivera, A., and Thomas, R.: Accelerated ice  
536 discharge from the Antarctic Peninsula following the collapse of Larsen B ice shelf, *Geophys*  
537 *Res Lett*, 31, Artn L1840110.1029/2004gl020697, 2004.

538 Rignot, E., Mouginot, J., and Scheuchl, B.: Ice Flow of the Antarctic Ice Sheet, *Science*, 333,  
539 1427-1430, 10.1126/science.1208336, 2011.

540 Rignot, E., Jacobs, S., Mouginot, J., and Scheuchl, B.: Ice-Shelf Melting Around Antarctica,  
541 *Science*, 341, 266-270, DOI 10.1126/science.1235798, 2013.

542 Rott, H., Skvarca, P., and Nagler, T.: Rapid collapse of northern Larsen Ice Shelf, *Antarctica*,  
543 *Science*, 271, 788-792, DOI 10.1126/science.271.5250.788, 1996.

544 Rott, H., Rack, W., Skvarca, P., and De Angelis, H.: Northern Larsen Ice Shelf, Antarctica:  
545 further retreat after collapse, *Annals of Glaciology*, Vol 34, 2002, 34, 277-282, Doi  
546 10.3189/172756402781817716, 2002.

547 Sasgen, I., Konrad, H., Ivins, E. R., Van den Broeke, M. R., Bamber, J. L., Martinec, Z., and  
548 Klemann, V.: Antarctic ice-mass balance 2003 to 2012: regional reanalysis of GRACE satellite  
549 gravimetry measurements with improved estimate of glacial-isostatic adjustment based on GPS  
550 uplift rates, *Cryosphere*, 7, 1499-1512, DOI 10.5194/tc-7-1499-2013, 2013.

551 Scambos, T., Hulbe, C., and Fahnestock, M.: Climate-induced ice shelf disintegration in the  
552 Antarctic Peninsula, *Antarct Res Ser*, 79, 79-92, 2003.

553 Scambos, T., Fricker, H. A., Liu, C. C., Bohlander, J., Fastook, J., Sargent, A., Massom, R.,  
554 and Wu, A. M.: Ice shelf disintegration by plate bending and hydro-fracture: Satellite  
555 observations and model results of the 2008 Wilkins ice shelf break-ups, *Earth Planet Sc Lett*,  
556 280, 51-60, 10.1016/j.epsl.2008.12.027, 2009.

557 Schroder, D., Feltham, D. L., Flocco, D., and Tsamados, M.: September Arctic sea ice  
558 minimum predicted by spring melt-pond fraction, *Nat Clim Change*, 4, 353-357,  
559 10.1038/Nclimate2203, 2014.

560 Spreen, G., Kaleschke, L., and Heygster, G.: Sea ice remote sensing using AMSR-E 89-GHz  
561 channels, *J Geophys Res-Oceans*, 113, Artn C02s0310.1029/2005jc003384, 2008.

562 Sugimoto, F., Tamura, T., Shimoda, H., Uto, S., Simizu, D., Tateyama, K., Hoshino, S., Ozeki,  
563 T., Fukamachi, Y., Ushio, S., and Ohshima, K. I.: Interannual variability in sea ice thickness in  
564 the pack-ice zone off Lutzow-Holm Bay, East Antarctica, *Polar Sci*, 10, 43-51,  
565 10.1016/j.polar.2015.10.003, 2016.

566 Todd, J., and Christoffersen, P.: Are seasonal calving dynamics forced by buttressing from ice  
567 melange or undercutting by melting? Outcomes from full-Stokes simulations of Store Glacier,  
568 West Greenland, *Cryosphere*, 8, 2353-2365, 10.5194/tc-8-2353-2014, 2014.

569 Ushio, S.: Factors affecting fast-ice break-up frequency in Lutzow-Holm bay, Antarctica,  
570 *Annals of Glaciology*, Vol 44, 2006, 44, 177-182, Doi 10.3189/172756406781811835, 2006.

571 van der Veen, C. J.: Calving glaciers, *Prog Phys Geog*, 26, 96-122,  
572 10.1191/0309133302pp327ra, 2002.

573 van Wessem, J. M., Reijmer, C. H., Morlighem, M., Mougintot, J., Rignot, E., Medley, B.,  
574 Joughin, I., Wouters, B., Depoorter, M. A., Bamber, J. L., Lenaerts, J. T. M., van de Berg, W.  
575 J., van den Broeke, M. R., and van Meijgaard, E.: Improved representation of East Antarctic  
576 surface mass balance in a regional atmospheric climate model, *J Glaciol*, 60, 761-770,  
577 10.3189/2014JoG14J051, 2014.

578 Wang, X., Holland, D. M., Cheng, X., and Gong, P.: Grounding and Calving Cycle of Mertz  
579 Ice Tongue Revealed by Shallow Mertz Bank, *The Cryosphere Discuss.*, 2016, 1-37,  
580 10.5194/tc-2016-3, 2016.

581 Wuite, J., Rott, H., Hetzenecker, M., Floricioiu, D., De Rydt, J., Gudmundsson, G. H., Nagler,  
582 T., and Kern, M.: Evolution of surface velocities and ice discharge of Larsen B outlet glaciers  
583 from 1995 to 2013, *Cryosphere*, 9, 957-969, 10.5194/tc-9-957-2015, 2015.

584 Yang, Y., Li, Z. J., Leppazranta, M., Cheng, B., Shi, L. Q., and Lei, R. B.: Modelling the  
585 thickness of landfast sea ice in Prydz Bay, East Antarctica, *Antarct Sci*, 28, 59-70,  
586 10.1017/S0954102015000449, 2016.

587 Young, D. A., Wright, A. P., Roberts, J. L., Warner, R. C., Young, N. W., Greenbaum, J. S.,  
588 Schroeder, D. M., Holt, J. W., Sugden, D. E., Blankenship, D. D., van Ommen, T. D., and  
589 Siegert, M. J.: A dynamic early East Antarctic Ice Sheet suggested by ice-covered fjord  
590 landscapes, *Nature*, 474, 72-75, 10.1038/nature10114, 2011.

591

592

593

594

595

596

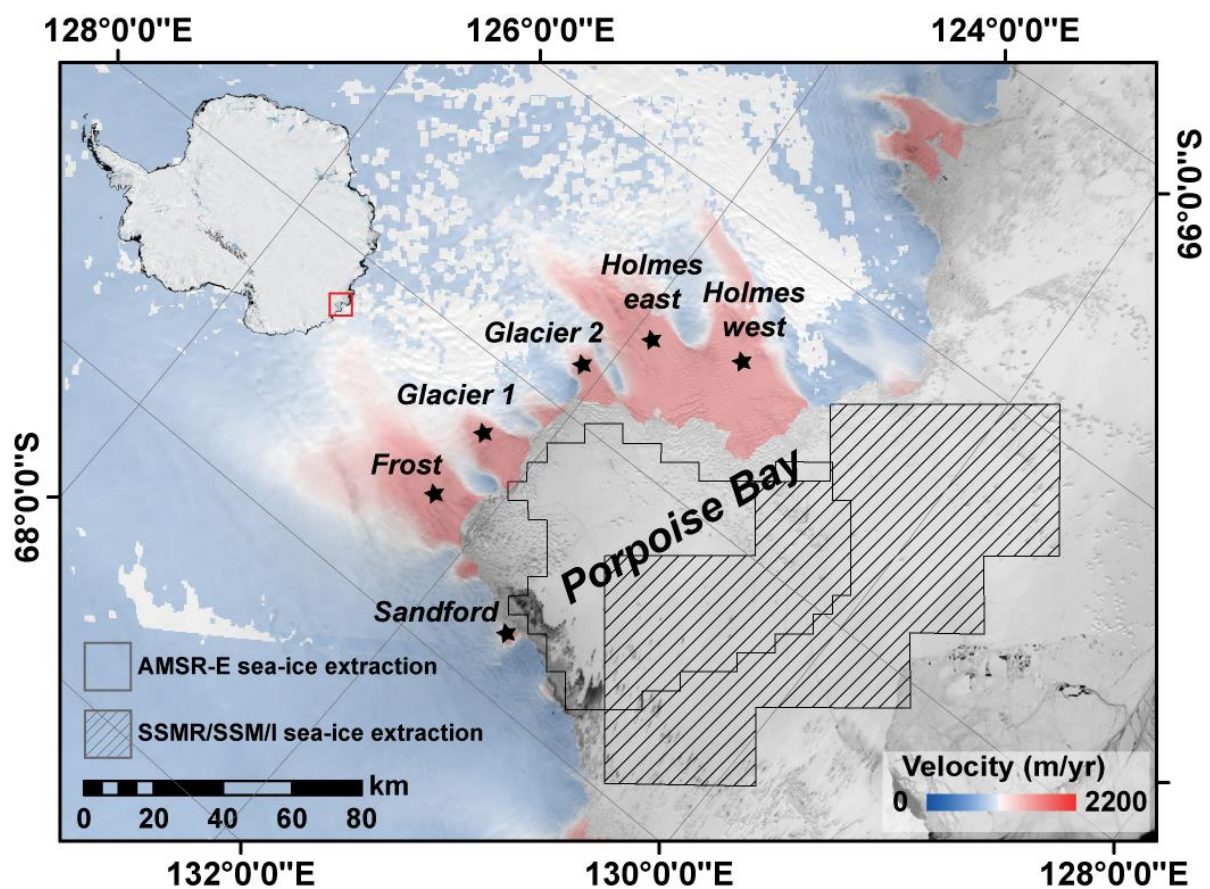
597

598 **Table 1: Satellite imagery used in the study**

Satellite	Date of Imagery
ARGON	October 1963 (Kim et al., 2007)
Envisat ASAR WSM	August 2002, November 2002 to March 2012 (monthly)
Landsat	January 1973; February 1991
MODIS	January 2001; December/January 2005/6; March 2016
RADARSAT	September 1997 (Liu and Jezek, 2004)
Sentinel-1	February-July, 2016

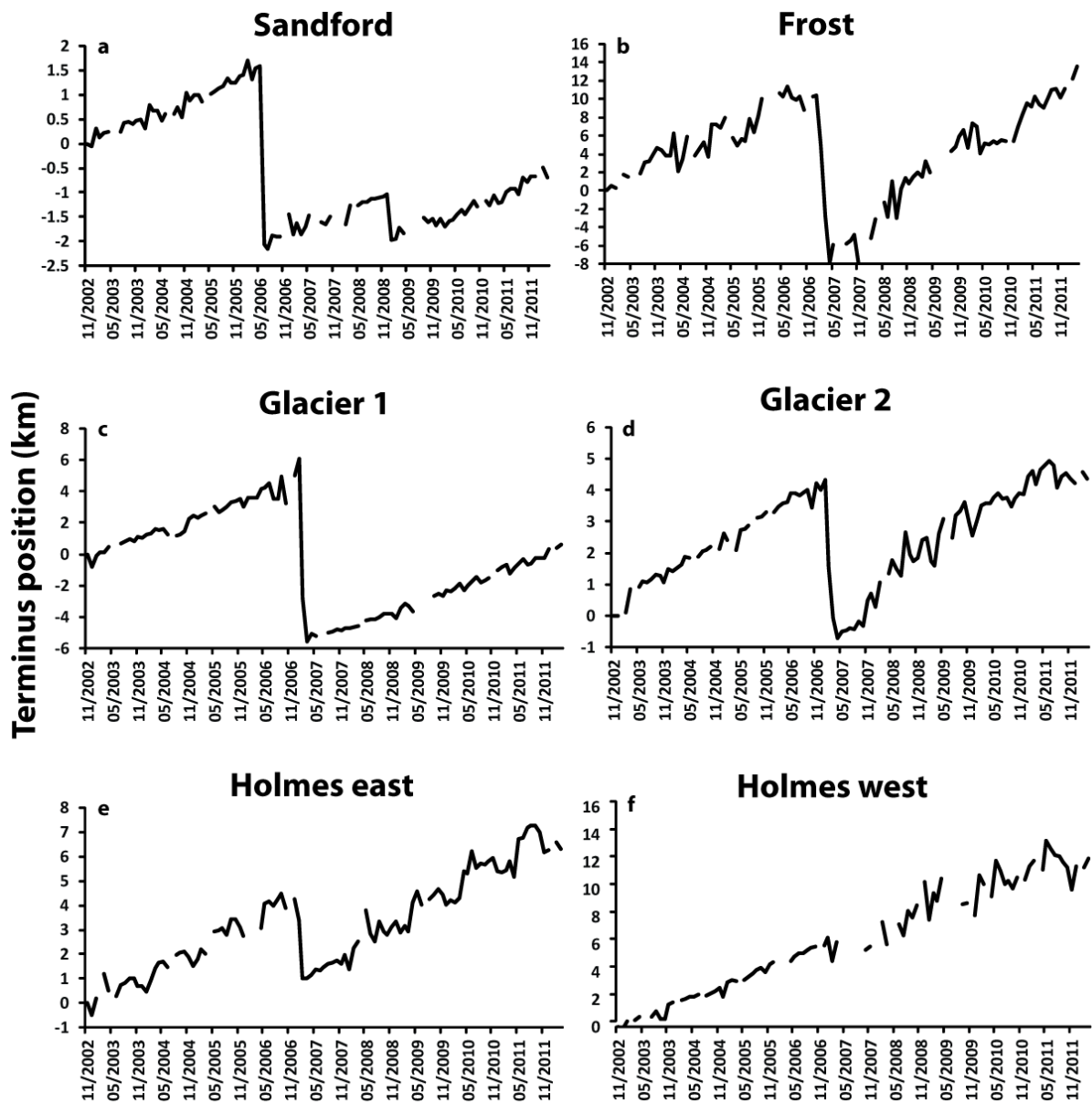
599

600



601

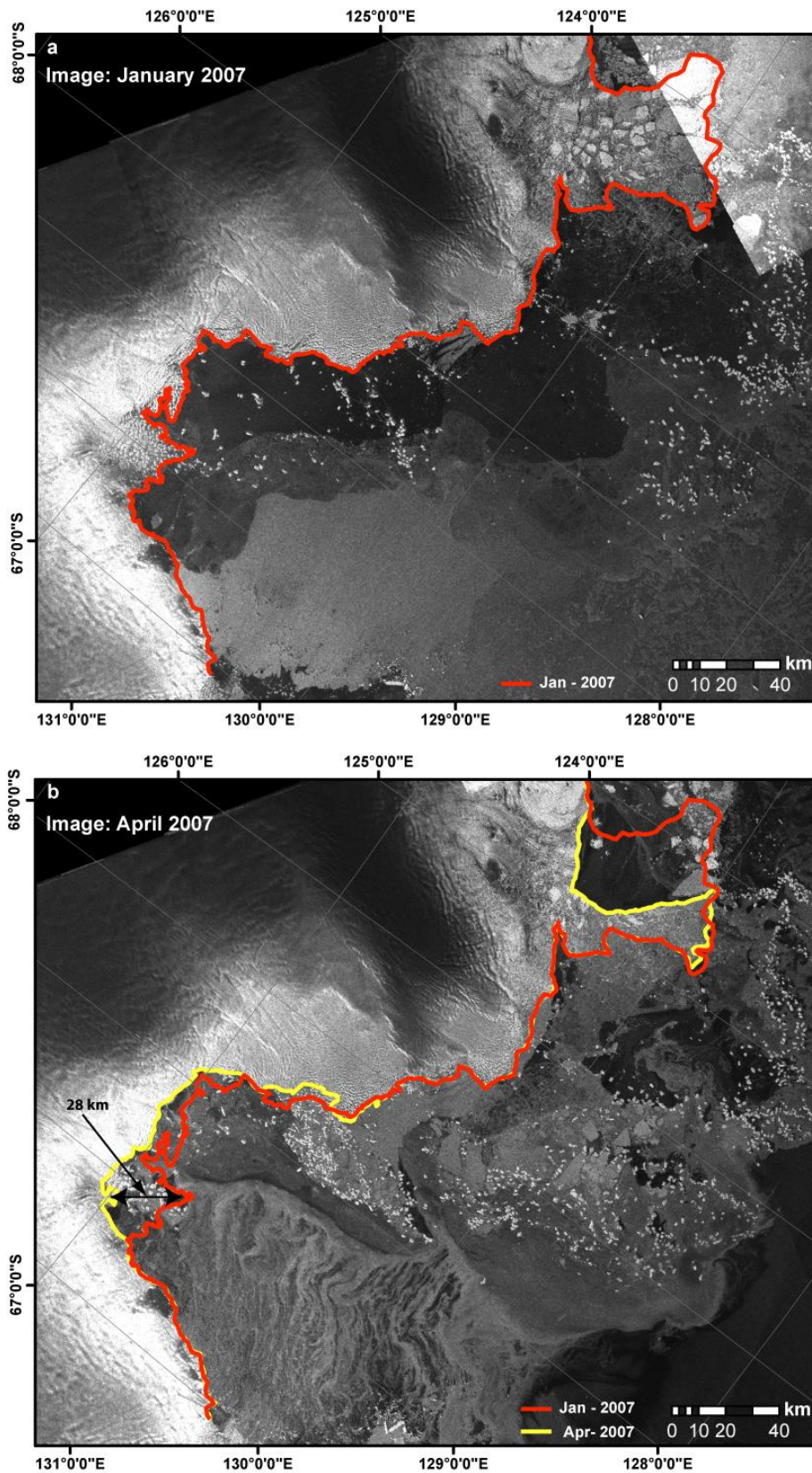
602 **Figure 1:** MODIS image of Porpoise Bay, with glacier velocities overlain (Rignot et al.,  
 603 2011). The hatched polygon represents the region where long-term 25 km resolution  
 604 SSMR/SSM/I sea ice concentrations were extracted. The non-hatched polygon represents the  
 605 region where the higher resolution (6.25 km) AMSR-E sea ice concentrations were extracted.



606

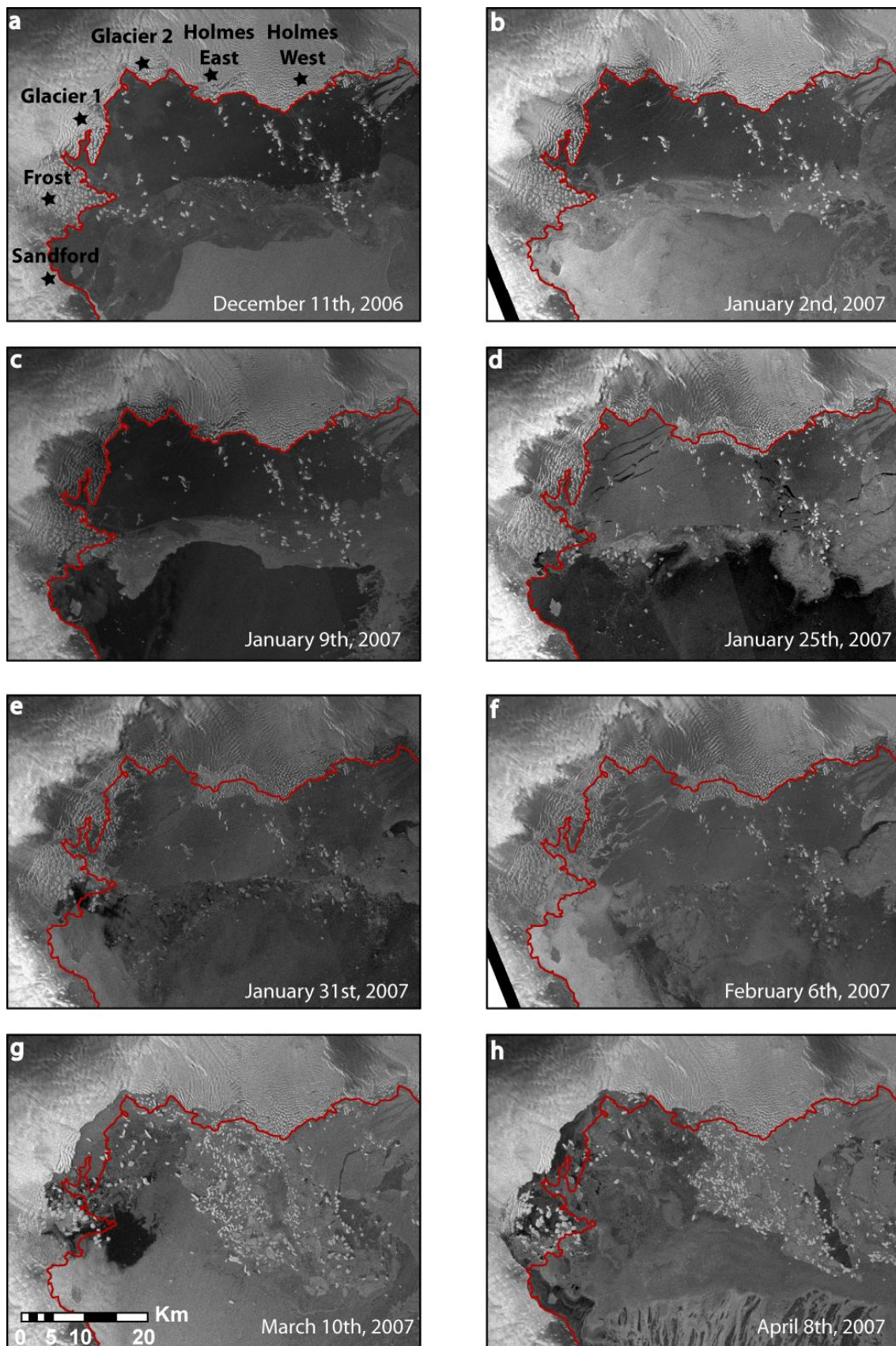
607 **Figure 2:** Terminus position change of six glaciers in Porpoise Bay between November 2002  
 608 and March 2012. Note the major calving event in January 2007 for 5 of the glaciers.

609 Terminus position measurements are subject to +/- 500 m. Note the different scales on y-axis.



610

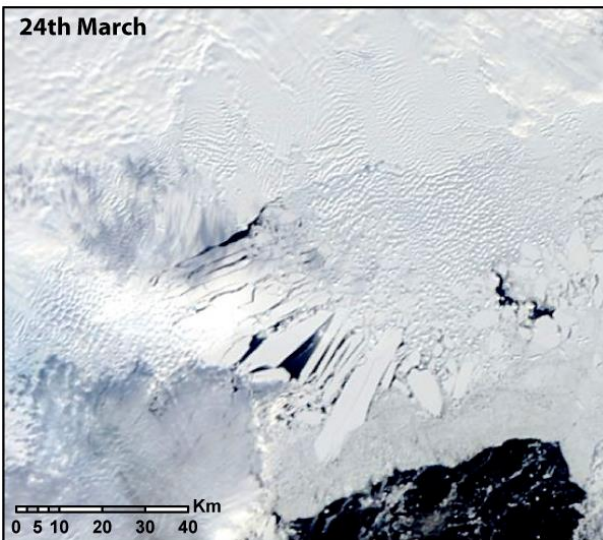
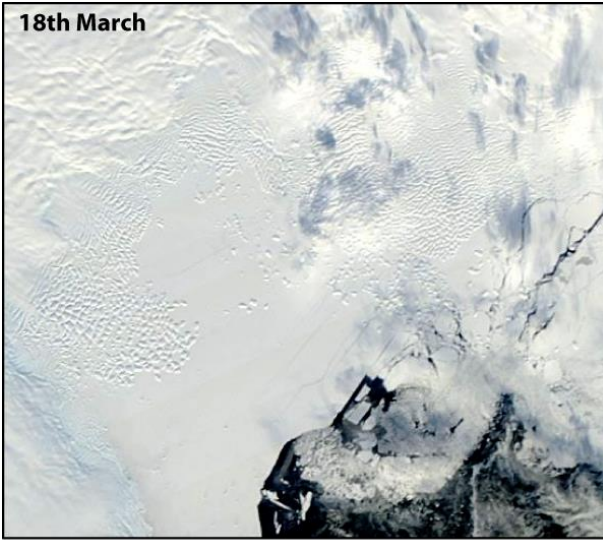
611 **Figure 3:** Envisat ASAR WSM imagery in January 2007 **a)** and April 2007 **b)**, which are  
 612 immediately prior to and after a near-simultaneous calving event in Porpoise Bay. Red line  
 613 shows terminus positions in January 2007 and yellow line shows the positions in April 2007.



614

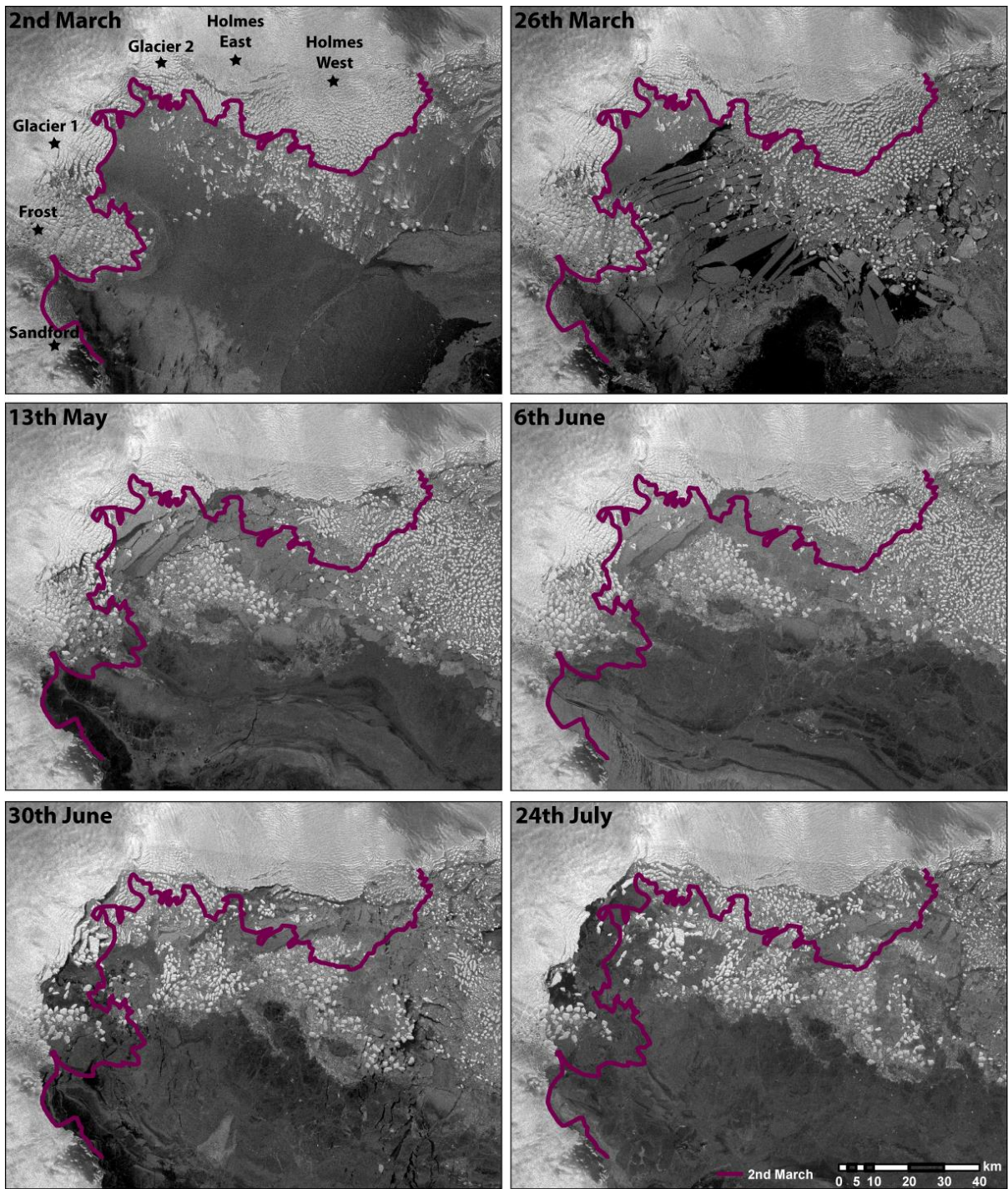
615 **Figure 4:** Envisat ASAR WSM imagery showing the evolution of the 2007 calving event.

616 Red line shows the terminus positions from December 11<sup>th</sup> 2006 on all panels.



617

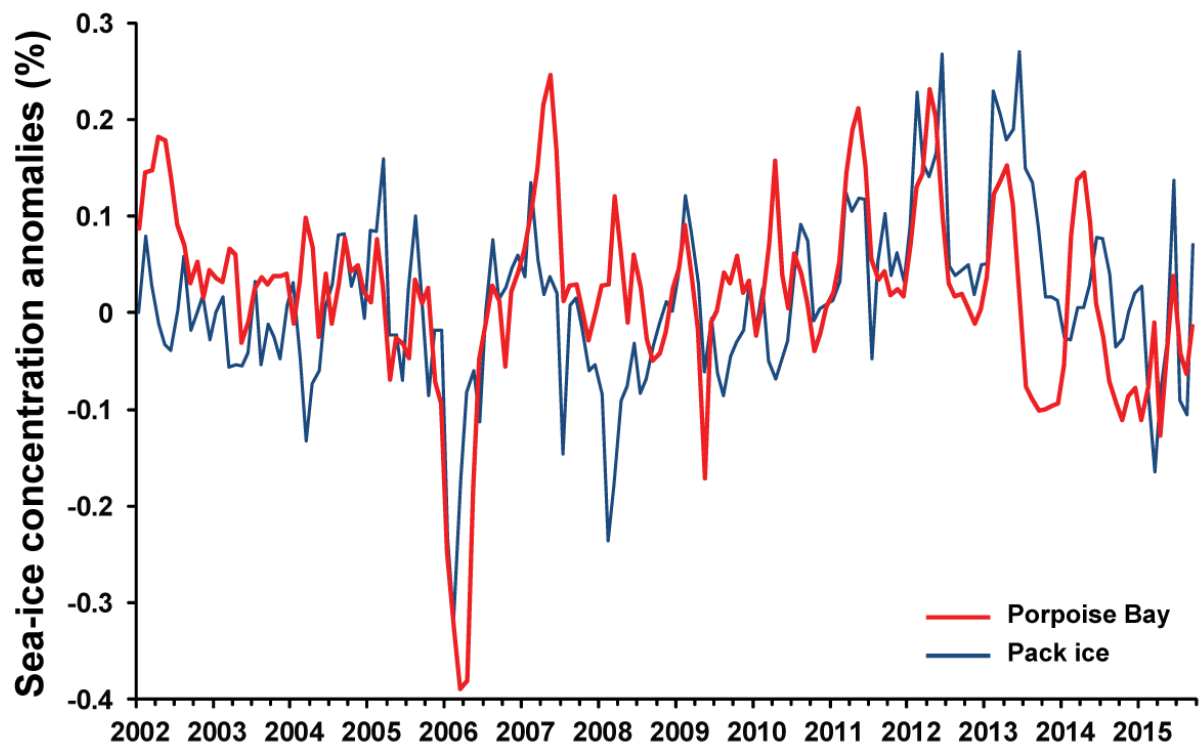
618 **Figure 5:** MODIS imagery showing the initial stages of disintegration of Holmes (West)  
619 Glacier in March 2016. On March 19<sup>th</sup> a large section of sea ice breaks away from the  
620 terminus (circled), initiating the rapid disintegration process. By the 24<sup>th</sup> March an 800 km<sup>2</sup>  
621 section of Holmes (West) Glacier tongue had disintegrated.



623

624 **Figure 6:** Sentinel-1 imagery showing the evolution of the 2016 calving event. Purple line  
625 shows the terminus position from 2<sup>nd</sup> March on all panels.





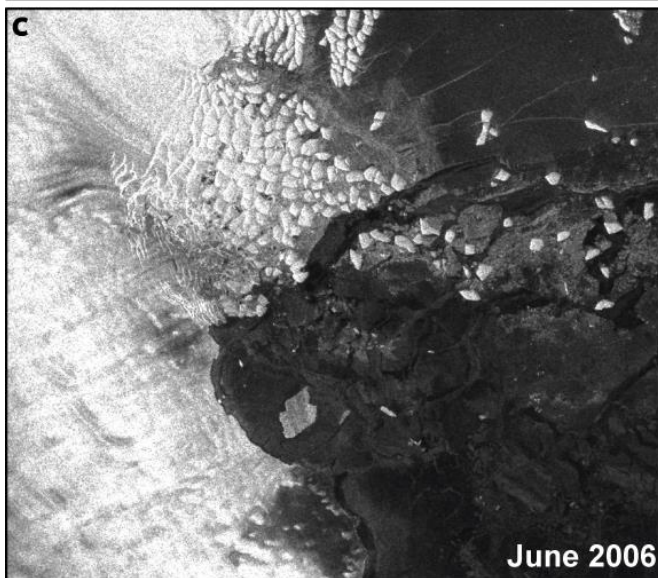
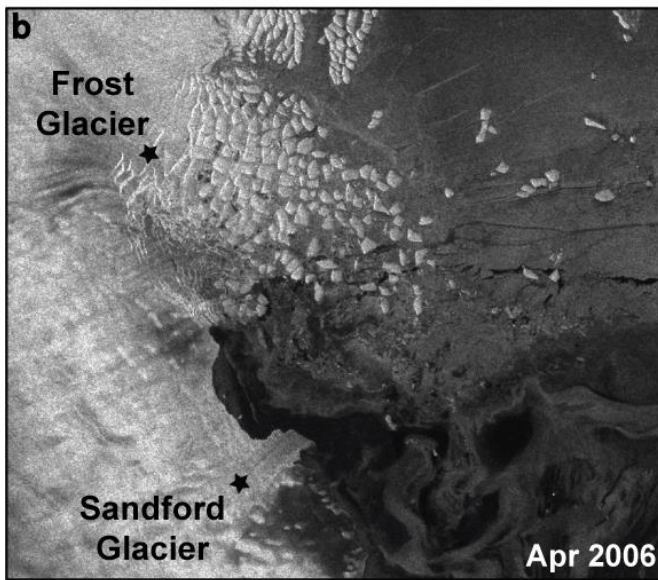
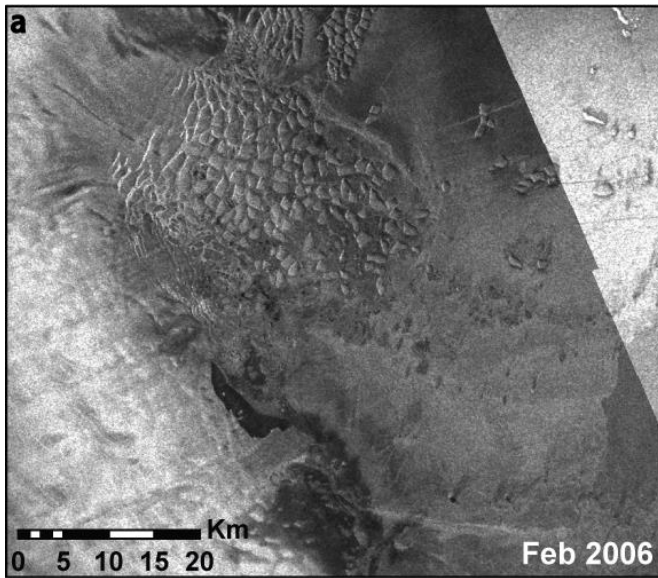
626

627 **Fig 7:** Mean monthly sea-ice-concentration anomalies from November 2002 to June 2016.

628 The red line indicates sea-ice-concentration anomalies in Porpoise Bay and the blue line

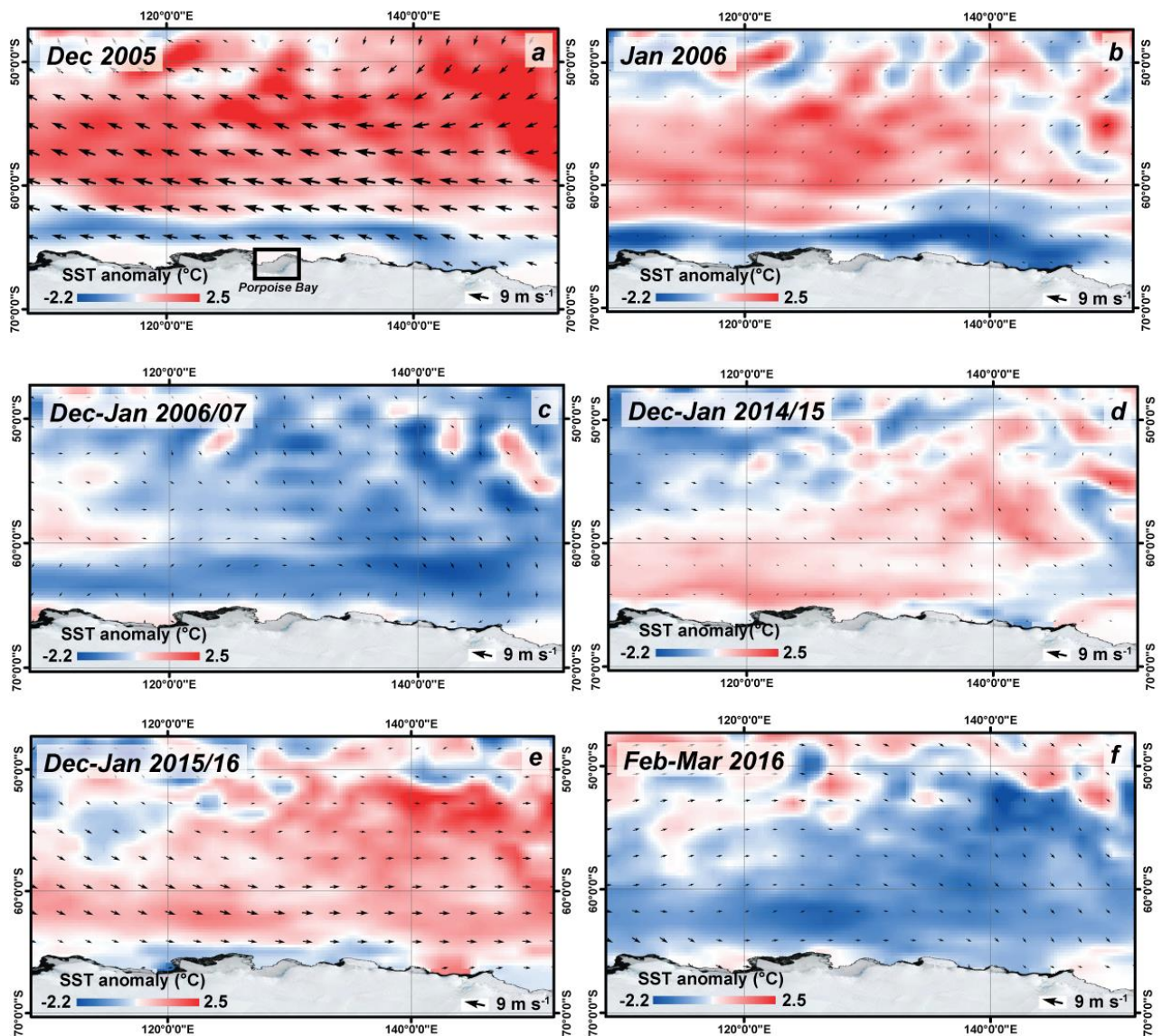
629 indicates pack-ice-concentration anomalies.

630



631

632 **Figure 8:** Time series of Frost and Sandford Glaciers calving showing that sea ice clears  
633 prior to calving and dispersal of icebergs.



634

635 **Figure 9:** Mean monthly ERA-Interim derived wind-field and sea-surface-temperature  
 636 anomalies in the months preceding the 2007 and 2016 sea ice break-ups. **a)** December 2005  
 637 **b)** January 2006 **c)** Mean December and January 2006/07 **d)** Mean December and January  
 638 2014/15 **e)** Mean December and January 2015/16 **f)** Mean February and March 2016.



639

640 **Figure 10:** Mean RACMO2.3-derived December melt 1979-2015 in Porpoise Bay.

641

642

643

644

645

646

647

648

649

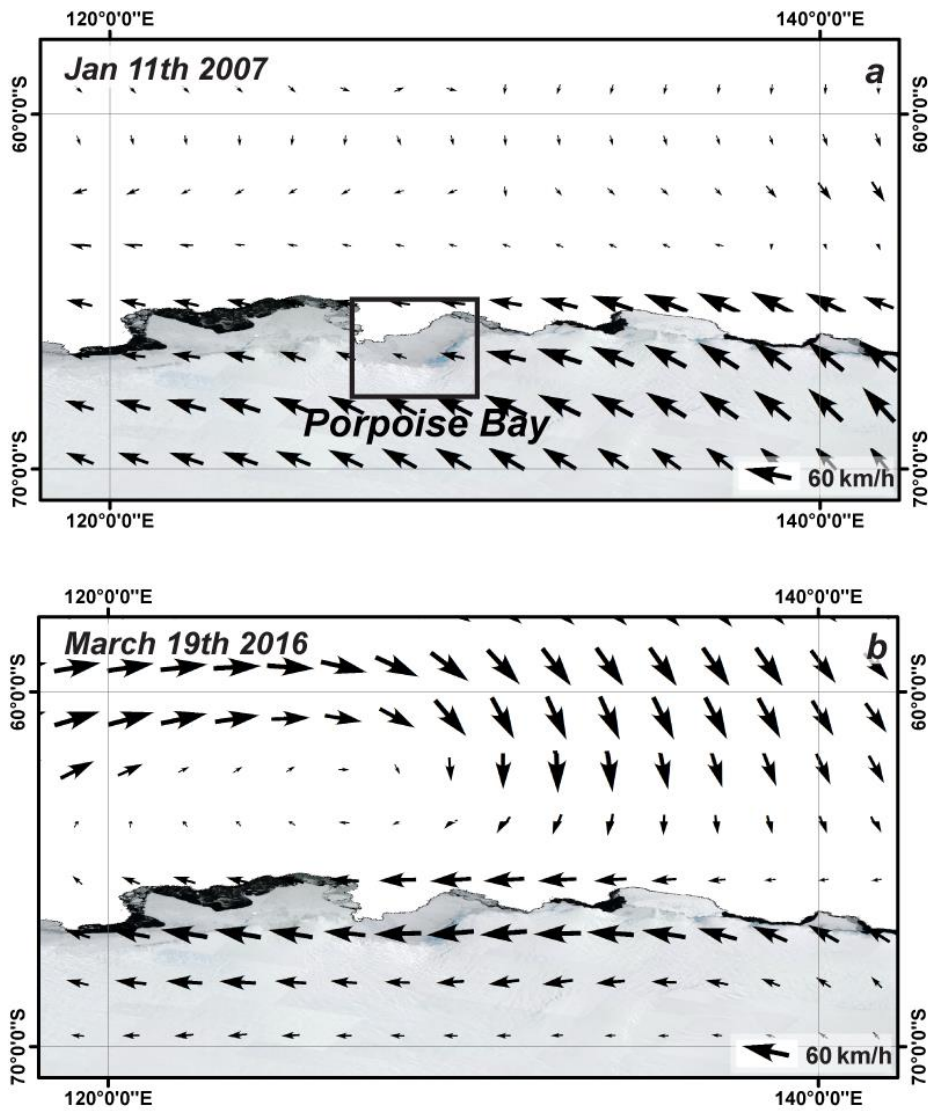
650

651

652

653

654



655

656 **Figure 11:** ERA-Interim derived wind fields for the estimated dates of sea ice break-up. **a)**  
 657 January 11<sup>th</sup> 2007 and **b)** March 19<sup>th</sup> 2016.

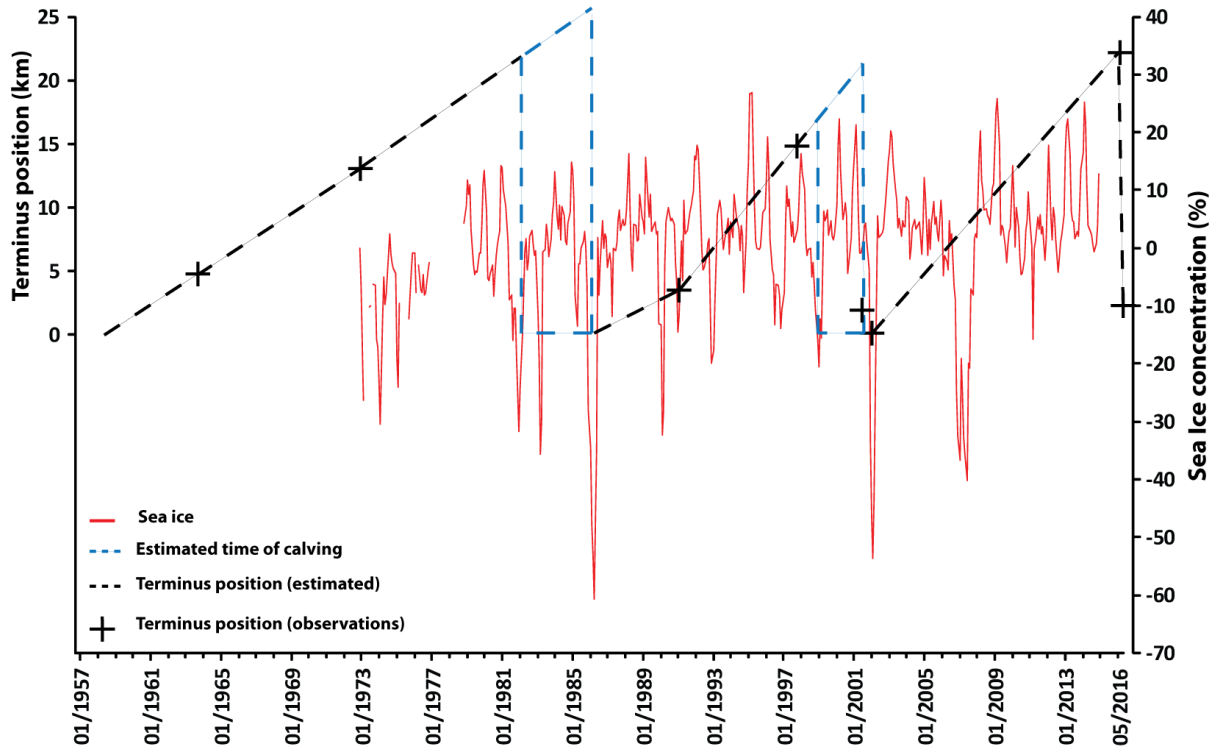
658

659

660

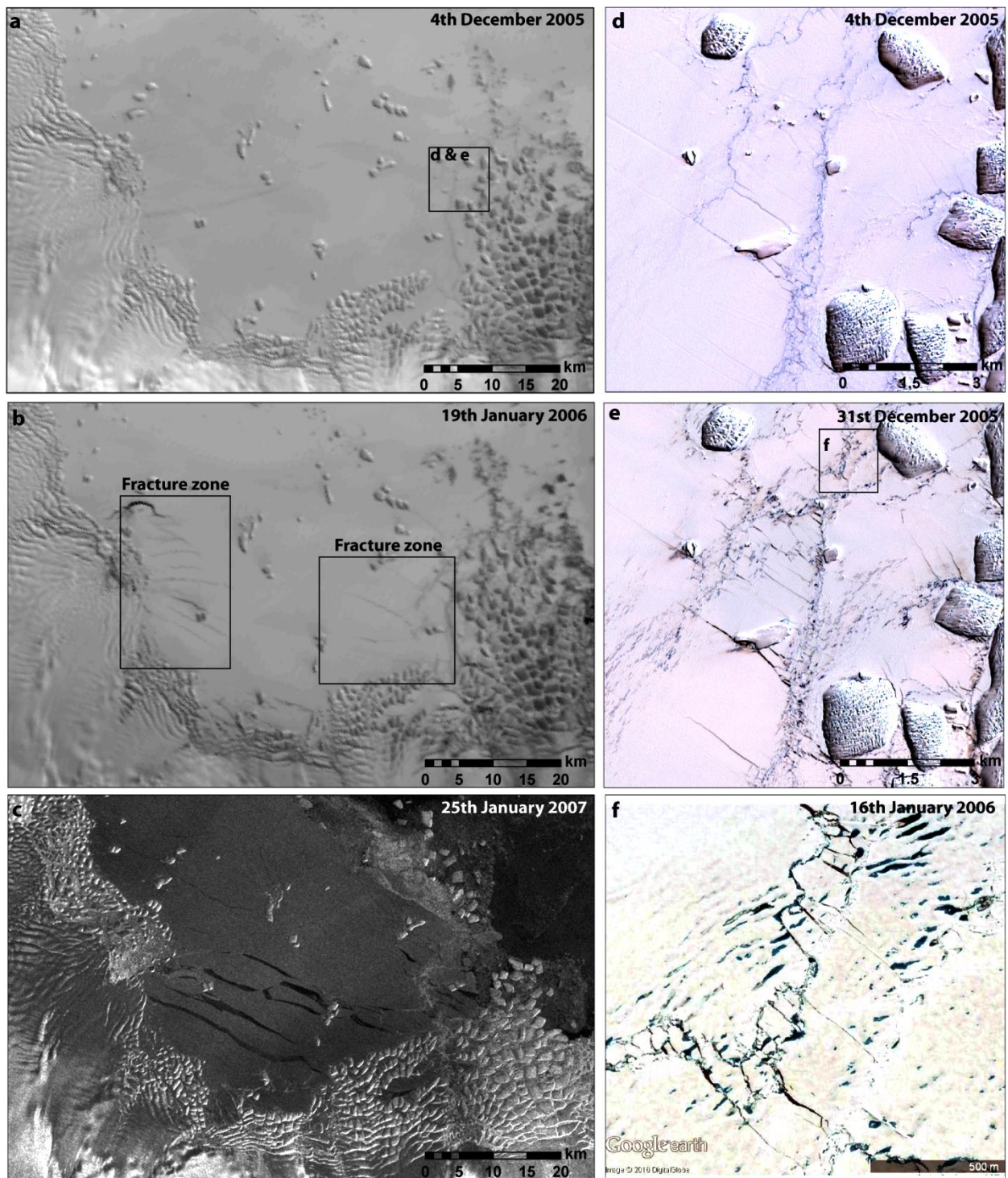
661

662



663  
 664 **Figure 12:** Reconstruction of the calving cycle of Holmes (West) Glacier. All observations  
 665 are represented by black crosses. The estimated terminus position is then extrapolated linearly  
 666 between each observation. In periods without observations the date of calving is estimated by  
 667 negative sea ice concentration anomalies.

668



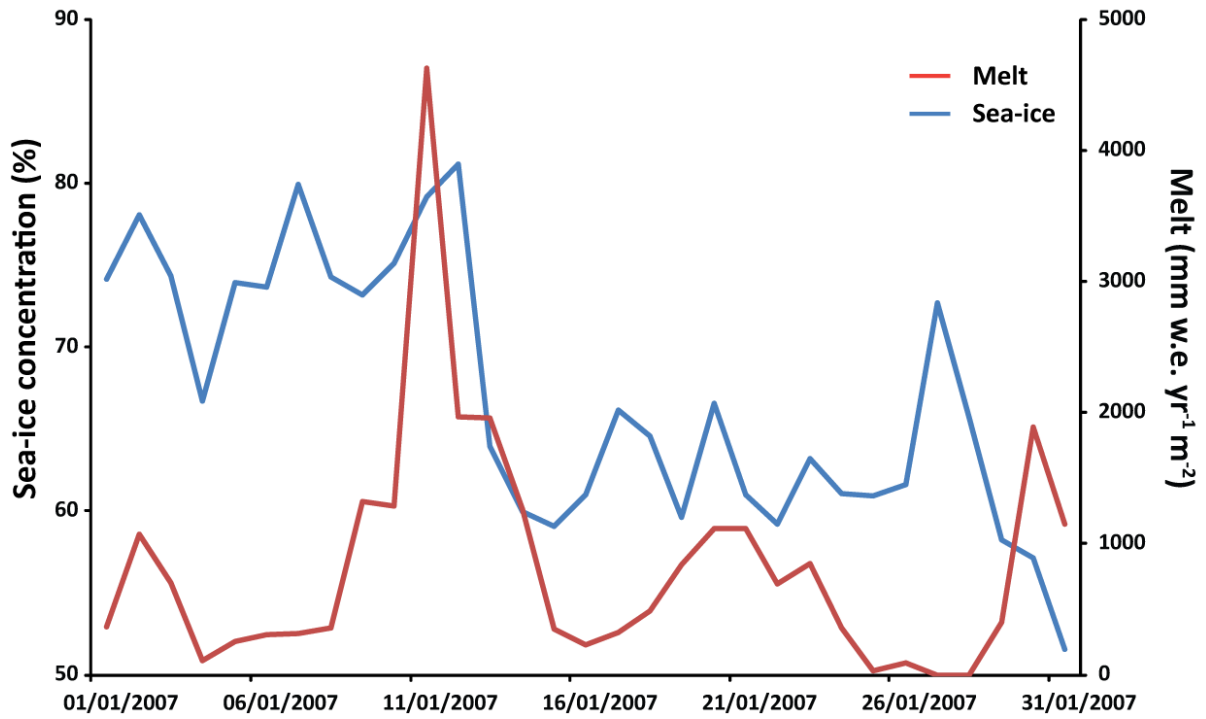
670

671 **Figure 13: a and b)** MODIS imagery showing the development of fractures in the landfast  
 672 sea ice between 4<sup>th</sup> December 2005 and 19<sup>th</sup> January 2006  
 673 (<http://dx.doi.org/10.7265/N5NC5Z4N>.) **c)** The landfast sea ice ruptures along some of the  
 674 same fractures which formed in December/January 2005/06, eventually leading to complete  
 675 break-up in January 2007. **d and e)** ASTER imagery showing surface melt features and the  
 676 development of smaller fracture between 4<sup>th</sup> and 31<sup>st</sup> December 2005. **f)** High resolution

677 optical satellite imagery from 16<sup>th</sup> January 2006 showing sea ice fracturing and surface melt  
678 ponding. This image was obtained from Google Earth.

679

680



681

682 **Figure 14:** Daily sea ice concentrations and RACMO2.3 derived melt during January 2007 in  
683 Porpoise Bay. Sea ice concentrations start to decrease after the melt peak on January 11<sup>th</sup>.

684

685

686

687

688

689

690

691